Chinese Journal of Chemical Engineering 64 (2023) 188–195

Contents lists available at ScienceDirect

Chinese Journal of Chemical Engineering

journal homepage: www.elsevier.com/locate/CJChE

Full Length Article

Insight into the green route to dimethyl succinate by direct esterification of bio-based disodium succinate using CO_2 and CH_3OH

Yu-Gao Wang *, Xiao-Chen Han, Bao Gu, Hua-Shuai Wu *, Jun Shen

School of Chemical Engineering and Technology, Taiyuan University of Technology, Taiyuan 030024, China

ARTICLE INFO

Article history:
Received 8 March 2023
Received in revised form 25 May 2023
Accepted 26 May 2023
Available online 18 August 2023

Keywords:
Succinate
Carbon dioxide
Direct esterification
Reaction mechanism
Reaction kinetics
Kinetic modeling

ABSTRACT

The fermentation for succinic acid production outperforms other methods by low energy consumption and environmental benignity, with the resulting products mainly as disodium succinate (DSA). By directly esterifying DSA using CO_2 and CH_3OH, it is expected to avoid the use of inorganic acids. By high-resolution mass spectrometry analysis and theoretical calculation, this study establishes that the reaction consists of three steps, *i.e.*, first forming 3-carboxypropanoate, then monomethyl succinate (MMS), and finally dimethyl succinate (DMS). A detailed kinetic analysis is further performed, the results demonstrate that the transformation of DSA to MMS is regarded to be a second-order reaction for reactant DSA, while the transformation of MMS to DMS is a first-order reaction for reactant MMS. The activation energy for the generation of MMS from DSA is 37.15 kJ·mol^{-1}, and that for the generation of DMS from MMS is 85.80 kJ·mol^{-1}, indicating the latter one is the rate-determining step.

1. Introduction

Succinic acid (SA) is an important synthetic intermediate for various chemicals and polymers [1,2]. The current industrial production of SA comes from the hydrogenation of maleic anhydride generated from the hydrogenation of petrochemical [3]. However, the large-scale production of SA from petrochemicals is inevitably limited by the fluctuating price and reserve of petroleum. Other than aligning with the current low-carbon economy [4], the biological synthesis of SA by the fermentation of lignocellulose and starch has the obvious advantages of low cost for the raw material and environmental benignity [5].

With intensifying public environmental awareness and enacting "plastic ban", the demand for biodegradable plastics such as poly(butylene succinate) is dramatically increasing [6]. As the starting material for synthesizing poly(butylene succinate), the production of SA and its homologous esters has become increasingly pressing [7]. Therefore, it is necessary to achieve stable and sustainable production of SA and dimethyl succinate (DMS) [8]. The polymerization of DMS by the current transesterification polymerization method [9] is a facile approach as compared with the direct melting polymerization [10] required for SA. Considering the polymerization method, DMS is an ideal polymer precursor [11]. The manufacture of desired chemicals from biomass is a very challenging task [12]. Under hypoxia conditions, corticium glutamate strains are required for producing SA [13]. During biological fermentation, a continuous addition of an alkaline solution is required to maintain the fermentation broth close to neutral [14], which is necessary for the efficient production of carboxylic acids [15] by microorganisms. Thus, the generated carboxylic acids in the fermentation tank are in the form of carboxylates [16], and the classical process of converting succinate to DMS usually involves the acidification of succinate to SA using inorganic acids and subsequent esterification with alcohols to generate DMS [17]. However, it is not environmentally benign during the acidification of succinate because a large amount of inorganic acid is consumed, thus generating a large amount of waste water.

The research group of Straathof used a strong anionic resin containing quaternary ammonium salt functional groups to adsorb succinate in the fermenter, and then directly produce DMS with chloroethane as a methylation reagent, greatly reducing the energy consumption and waste production [18]. However, chloride compounds as reagents do not comply with the policy of environmental protection. So direct esterification has been upgraded by replacing chloroethane with benign dimethyl carbonate (DMC) [19,20]. Nevertheless, the current production cost of DMC is relatively high [21]. It is urgent to reduce CO_2 emissions, because excessive CO_2 emissions disrupt the natural carbon cycle balance,

* Corresponding authors.
E-mail addresses: wangyugao@tyut.edu.cn (Y.-G. Wang), wuhuashuai@tyut.edu.cn (H.-S. Wu).

https://doi.org/10.1016/j.cjche.2023.05.017
1004-9541/

also aggravate global warming and natural disasters [22–24]. Meanwhile, CO_2 is a valuable C1 resource, the capture [25], storage [26], and utilization [27] of CO_2 have been attracted increasing attention. CO_2 and methanol could be used for synthesizing DMC [28–30]. Straathof *et al.* [31] adopted CO_2 and methanol as esterification reagents, achieved the direct esterification of succinate, and realized the fixation of CO_2 to a certain extent. Moreover, the formed carbonate as a byproduct could be recycled into the fermenter to maintain the fermentation broth close to neutral. The recent work of Straathof's research group [31] greatly facilitated the direct esterification of succinate. However, due to the inherent instability of ion exchange resin, the esterification of succinate was only conducted at a low reaction temperature (<100 °C), resulting in only an 18% mole yield of DMS after 20 h.

In the absence of resin, Kulkarni *et al.* [32] have achieved the direct esterification of some monocarboxylates at high temperature (170–175 °C) with CO_2 and methanol as esterification reagents for the first time. The yields of methyl acetate and methyl lactate reached up to 81% and 81.2% only after 5 h, respectively. Furthermore, it is worth investigating the application of this method for the direct esterification of succinate.

Based on the current research progress, this study would focus on the direct esterification of bio-based dicarboxylates using CO_2 and methanol as esterification reagents. With disodium succinate (DSA) as a model compound, the reaction conditions, reaction mechanism and kinetics in the direct esterification process were investigated by high resolution mass spectrometry (HRMS), theoretical calculations and simulation.

2. Materials and Methods

2.1. Materials

The majority of reagents were used as analytically pure, such as SA (>98.0%), DSA (>99.0%), CH_3OH (99.5%), monomethyl succinate (MMS) (>98.0%), and DMS (99.0%). Acetonitrile was chromatographically pure. Phosphoric acid was used at 85% (mass), hydrochloric acid at 36% (mass) and the purity of CO_2 was greater than 99.9%. Deionized water was used for all reactions.

2.2. Experimental section

As displayed in Fig. 1, DSA was dissolved in 50 ml CH_3OH, and then transferred into a 250 ml stainless-steel, magnetically stirred autoclave. The solution inside the autoclave was purged with CO_2 three times, and the autoclave was pressurized with CO_2 to a desired pressure at room temperature, heated to an indicated temperature within 30 min, and maintained for different time. Then the autoclave was immediately cooled to room temperature in an ice water bath. The resulted mixture in the autoclave was subjected to HRMS and high performance liquid chromatography (HPLC) analysis.

2.3. Analytical methods

The qualitative analysis of the product was conducted by HRMS of Bruker solariX 70 (Germany), equipped with an electrospray ionization source in positive and negative modes. The moisture content in the reaction sample before and after the reaction was analyzed by the Karl Fisher titration method using automatic Karl Fischer instrument (Metrohm AG, Switzerland).

For the chromatographic analysis, the mixture of the reaction products was acidified, and the amount of SA was used to indicate the amount of DSA in the reaction. The quantitative analysis was conducted with Agilent 1260 high performance liquid chromatography (HPLC) with ZORBAX SB-C18 chromatographic column (5 μm × 4.6 mm × 250 mm). The mobile phase was acetonitrile and 0.10% phosphoric acid aqueous solution. The flow rate was set at 1.0 ml·min^{-1}. The UV detection wavelength was 210 nm. The injection volume was 20 μl, and the column temperature was 35 °C. The eluent containing SA, MMS and DMS was detected by the gradient elution program, and the standard liquid chromatography and the corresponding linear relationship were shown in Fig. 2 and Table 1. The products were quantitatively analyzed *via* HPLC by using the external standard method. The conversion rate of DSA, the yield and the selectivity of MMS and DMS were calculated as follows (unit of amount: mol):

$$\text{Conversion of DSA} = \frac{\text{initial amount of DSA} - \text{detect amount of SA}}{\text{initial amount of DSA}}$$

$$\text{Yield of MMS} = \frac{\text{amount of MMS generated}}{\text{inital amount of DSA}}$$

$$\text{Yield of DMS} = \frac{\text{amount of DMS generated}}{\text{inital amount of DSA}}$$

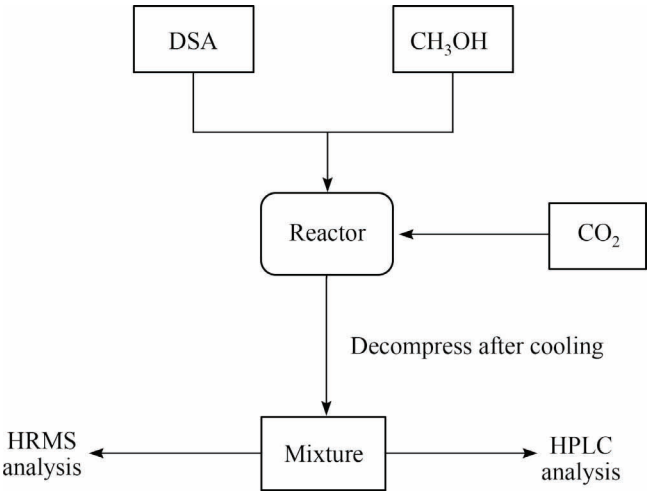

Fig. 1. Experimental procedure of esterification reaction of DSA, CH_3OH and CO_2.

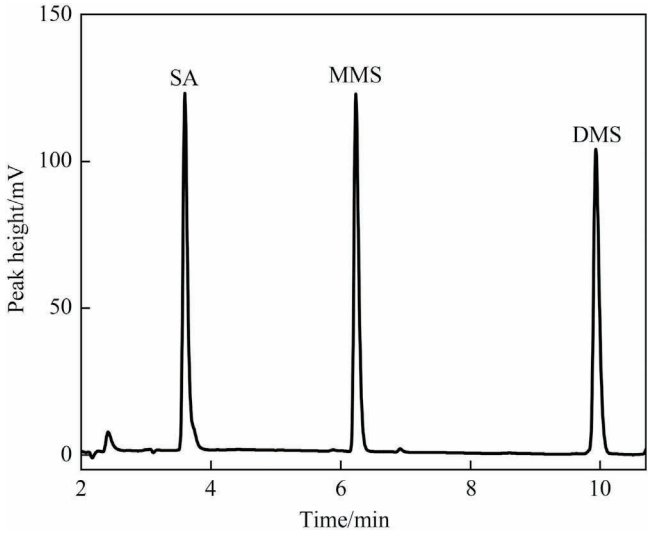

Fig. 2. HPLC spectrum of pure SA, MMS and DMS.

Table 1
Parameters for external standard curves of SA, MMS and DMS in HPLC analysis

Sample	Retention time/min	Linear equation	R^2
SA	3.60	y = 1.6796x–22.184	0.9991
MMS	6.22	y = 1.6305x–17.069	0.9994
DMS	9.95	y = 1.6668x–14.574	0.9993

$$\text{Selectivity of MMS} = \frac{\text{amount of MMS generated}}{\text{amount of product}}$$

$$\text{Selectivity of DMS} = \frac{\text{amount of DMS generated}}{\text{amount of product}}$$

3. Results and Discussion

3.1. Influence of reaction conditions on the direct esterification of DSA

The reaction temperature is a dictating factor for the esterification reaction. As shown in Fig. 3(a), the conversion rate of DSA increased first and then approached steady with increasing reaction temperature. Before the reaction temperature reached 150 °C, the yield of MMS in the system increased rapidly and then decreased gradually with the increased temperature. The yield of DMS increased with raising reaction temperature, but the increasing rate was faster at the temperature higher than 160 °C. The data indicated that the reaction temperature within a certain range would facilitate the conversion rate of DSA, and the increase of temperature was conducive to the conversion of MMS to DMS, which could be attributed to that more MMS were activated to cross the reaction barrier to form the product DMS at the high temperature. The yield of DMS gradually increased, while the yield of MMS initially increased to the maximum and then decreased with the reaction time evolution in Fig. 3(b). As shown in Fig. 3(c), the conversion rate of DSA and the yield of MMS gradually increased with the elevating initial pressure of CO_2, while the yield of DMS remained basically unchanged, which suggested that the increased initial pressure of CO_2 could only increase the conversion of DSA to MMS. This might be due to that the equilibrium shifted to the precursor of MMS from DSA at the high initial pressure of CO_2, which resulted in the increased yield for MMS. As displayed in Fig. 3(d), the conversion rate of DSA and the yield of MMS and DMS gradually decreased, but the selectivity of DMS almost remained constant with the increased addition of DSA. It was suggested that the initial concentration of DSA maybe not be involved in the rate equation, or this reaction was not the rate-determining step for the final product of DMS.

3.2. Reaction pathways for the direct esterification of DSA

For the determination of reaction pathways, it is important to first determine the specific distribution of the products. The crude reaction mixture from the reaction of DSA with CH_3OH and CO_2 consisted of carboxylic acid ester, carboxylic acid, and carboxylate, and it was difficult to be directly analyzed by HPLC or gas chromatography/mass spectrometry. HRMS could achieve the product self-separation and then analyze the components with high resolu-

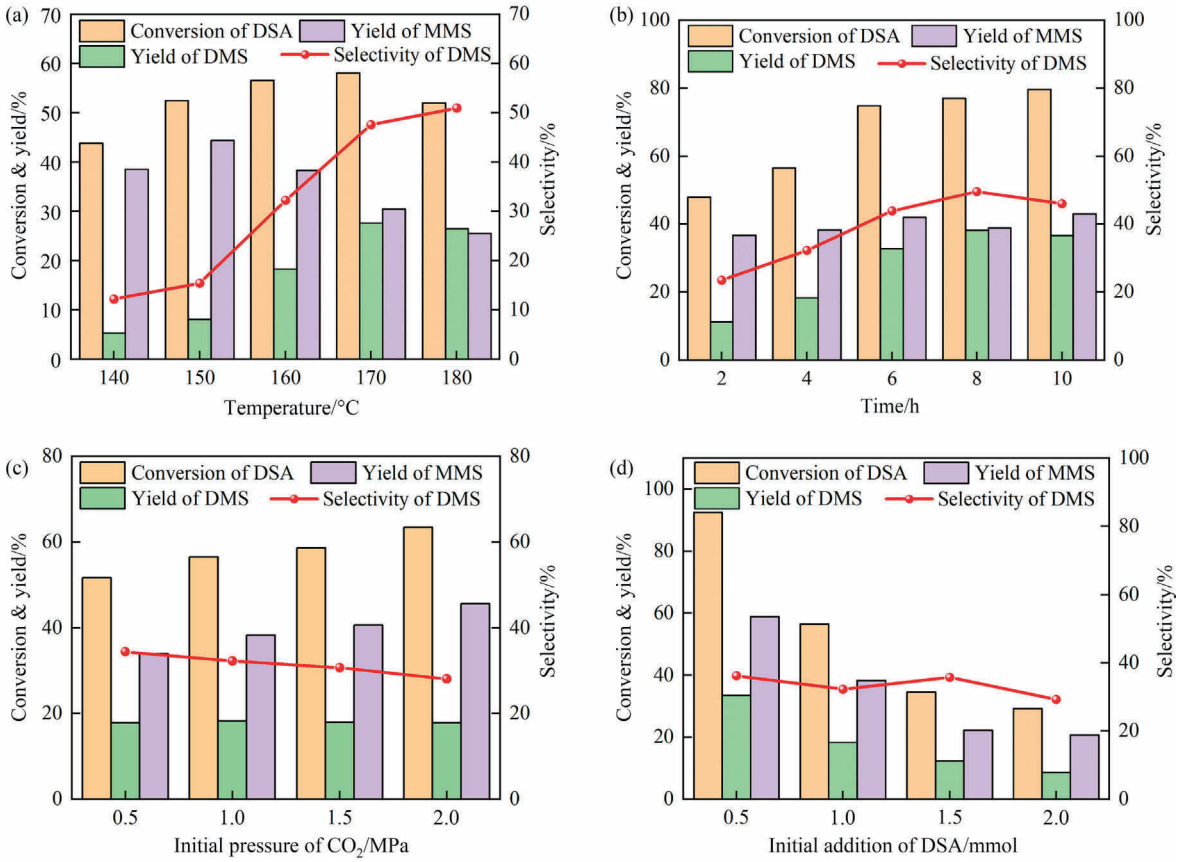

Fig. 3. Reaction conditions for the conversion of DSA, yields of MMS and DMS and selectivity of DMS in DSA esterification reaction (reaction conditions: (a) reaction time 4 h, initial pressure of CO_2 1.0 MPa, initial DSA dosage 1.0 mmol; (b) reaction temperature 160 °C, initial CO_2 pressure 1.0 MPa, initial DSA addition 1.0 mmol; (c) reaction temperature 160 °C, reaction time 4 h, DSA initial dosage 1.0 mmol; (d) reaction temperature 160 °C, reaction time 4 h, initial pressure of CO_2 1.0 MPa).

tion. Also, the molecular composition of each component in the product mixture could be inversely derived from the accurate molecular weight. In this study, the resulting mixture from the direct esterification of DSA with CH_3OH and CO_2 was directly analyzed by HRMS. As shown in Fig. 4 and Table 2, some components were determined, which were DMS (Compound 1), sodium 4-methoxy-4-oxobutanoate (Compound 2), DSA (Compound 3), methyl carbonate (Compound 4), MMS (Compound 5), 3-carboxypropionate (Compound 6), and sodium 3-carboxypropanoate (Compound 7).

On the basis of HRMS analysis, it was proposed that the process of DSA direct esterification reaction. Diphenyldiazomethane has been reported as an active probe to intercept acidic substances generated in alcohol solution under CO_2 atmosphere, for verifying the generation of alkylcarbonic acid [33]. Then, the formation and dissociation of alkyl carbonates in alcohol and CO_2 systems were determined by UV spectroscopy [34]. The results indicated that CO_2 reacted with methanol and formed alkylcarbonic acid, which then dissociated to free H^+. In this study, a large amount of CO_2 and CH_3OH were in the reaction system, thus, CO_2 and CH_3OH could react to form methyl carbonic acid, then dissociate to release H^+ as shown in Eqs. (1) and (2), which were further confirmed by the presence of methyl carbonate (Compound 4) in the product mixture detected by HRMS. The conductivity of CH_3OH was 2.43 $\mu S \cdot cm^{-1}$, but the conductivity of the reaction mixture system reached up to about 800 $\mu S \cdot cm^{-1}$ after adding 0.50–2.0 mmol DSA, which evidenced the dissociation of DSA in CH_3OH as displayed in Eq. (3). Meanwhile, a trace amount of water in CH_3OH could be reduced by reacting with CO_2 to generate carbonic acid and release H^+, which could be confirmed by decreasing water content from 0.15% to 0.04% by Karl Fischer method. Monosodium monosuccinate dissociated from DSA possibly associated with H^+ released from methyl carbonic acid to produce sodium 3-carboxypropanoate (Compound 7), which was detected by HRMS as shown in Eq. (4).

$$CO_2 + CH_3OH \rightleftharpoons CH_3OCOOH \quad (1)$$

$$CH_3OCOOH \rightleftharpoons \underset{4}{CH_3OCOO^-} + H^+ \quad (2)$$

$$\underset{3}{\begin{matrix}CH_2COONa\\ |\\ CH_2COONa\end{matrix}} \rightleftharpoons \begin{matrix}CH_2COO^-\\ |\\ CH_2COONa\end{matrix}^+ + Na^+ \quad (3)$$

$$\begin{matrix}CH_2COO^-\\ |\\ CH_2COONa\end{matrix}^+ + H^+ \rightleftharpoons \underset{7}{\begin{matrix}CH_2COOH\\ |\\ CH_2COONa\end{matrix}} \rightleftharpoons \underset{6}{\begin{matrix}CH_2COOH\\ |\\ CH_2COO^-\end{matrix}} + Na^+ \quad (4)$$

There would be two reaction paths for the subsequent reaction of 3-carboxypropanoate (Compound 7). 3-Carboxypropanoate might react with CH_3OH to generate sodium 4-methoxy-4-oxobutanoate (Compound 2), and then Compound 2 could further react with H^+ to form MMS. Alternatively, 3-carboxypropanoate might react with CH_3OH to directly form MMS. To certify the reaction path of 3-carboxypropanoate, the theoretical calculation with Gaussian 16 was conducted to optimize the structure of compounds by the B3LYP method of density functional theory for the most stable molecular structures and the thermodynamic parameters. It was found that at the reaction conditions of 140 °C and 3.1 MPa, ΔG was 143.09 $kJ \cdot mol^{-1}$ for the direct generation of MMS from 3-carboxypropanoate and CH_3OH, suggesting that this process cannot occur under these reaction conditions. But it was thermodynamically favorable (ΔG = − 10.89 $kJ \cdot mol^{-1}$) to form sodium 4-methoxy-4-oxobutanoate (Compound 2) from 3-carboxypropanoate and CH_3OH under the same conditions. Therefore, the theoretical calculation along with HRMS results suggested that 3-carboxypropanoate first reacted with CH_3OH to generate 4-methoxy-4-oxobutanoate (Compound 2), and then Compound 2 reacted with H^+ to generate MMS, as summarized in Eqs. (5) and (6). The high pressure of CO_2 could expedite the formation of 3-carboxypropanoate (Compound 7) from DSA by shifting the chemical equilibrium, and 3-carboxypropanoate (Compound 7) was the precursor for MMS generation. Therefore, MMS generation was increased at the high pressure of CO_2.

$$\underset{7}{\begin{matrix}CH_2COOH\\ |\\ CH_2COONa\end{matrix}} + CH_3OH \longrightarrow \underset{2}{\begin{matrix}CH_2COOCH_3\\ |\\ CH_2COONa\end{matrix}} + H_2O \quad (5)$$

$$\underset{2}{\begin{matrix}CH_2COOCH_3\\ |\\ CH_2COONa\end{matrix}} + H^+ \longrightarrow \underset{5}{\begin{matrix}CH_2COOCH_3\\ |\\ CH_2COOH\end{matrix}} + Na^+ \quad (6)$$

In Fig. 5, the mole fraction of SA decreased, and the mole fraction of MMS increased first and then decreased, but the mole fraction of DMS increased gradually with the reaction time evolution. Meanwhile, the selectivity of MMS decreased and the selectivity of DMS increased gradually, which was consistent with the feature of continuous reaction [35]. In other words, the formed MMS fur-

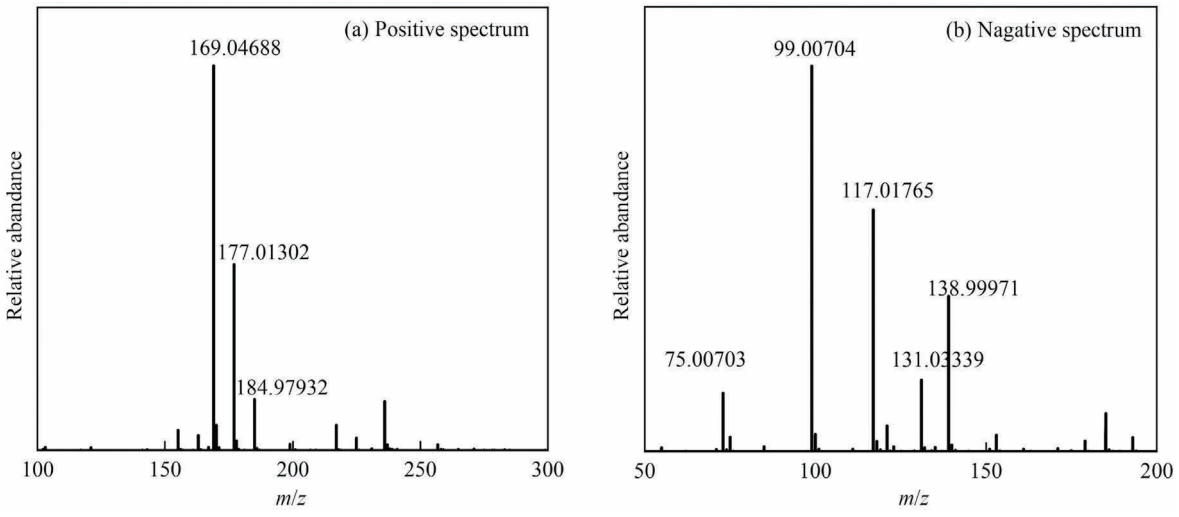

Fig. 4. HRMS spectra of the crude reaction mixture after reaction (reaction conditions: reaction temperature 160 °C, reaction time 2 h, initial CO_2 pressure 1.0 MPa, DSA addition 1.0 mmol).

Table 2
Possible molecular formulas obtained by HRMS detection of the resulting mixture after reaction

Sample	Presumed molecular formula	Presumed compound	Possible structure of the compound	*m/z*		ESI source
				Measured value	Theoretical value	
1	$C_6H_{10}NaO_4$	DMS	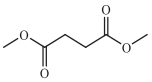	169.04688	[146.05791 + Na] $^+$	+
2	$C_5H_7Na_2O_4$	Sodium 4-methoxy-4-oxobutanoate	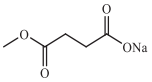	177.01302	[154.02421 + Na] $^+$	
3	$C_4H_4Na_3O_4$	DSA	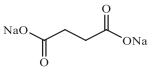	184.97932	[161.99049 + Na] $^+$	
4	$C_2H_3O_3^-$	Methyl carbonate		75.00703	75.00822	–
5	$C_5H_7O_4$	Monomethyl succinate	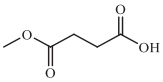	131.03339	[132.04225-H]$^-$	
6	$C_4H_5O_4^-$	3-Carboxypropanoate	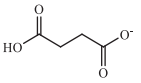	117.01765	117.01878	
7	$C_4H_4NaO_4$	Sodium 3-carboxypropanoate	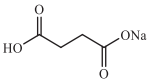	138.90389	[139.00073-H]$^-$	

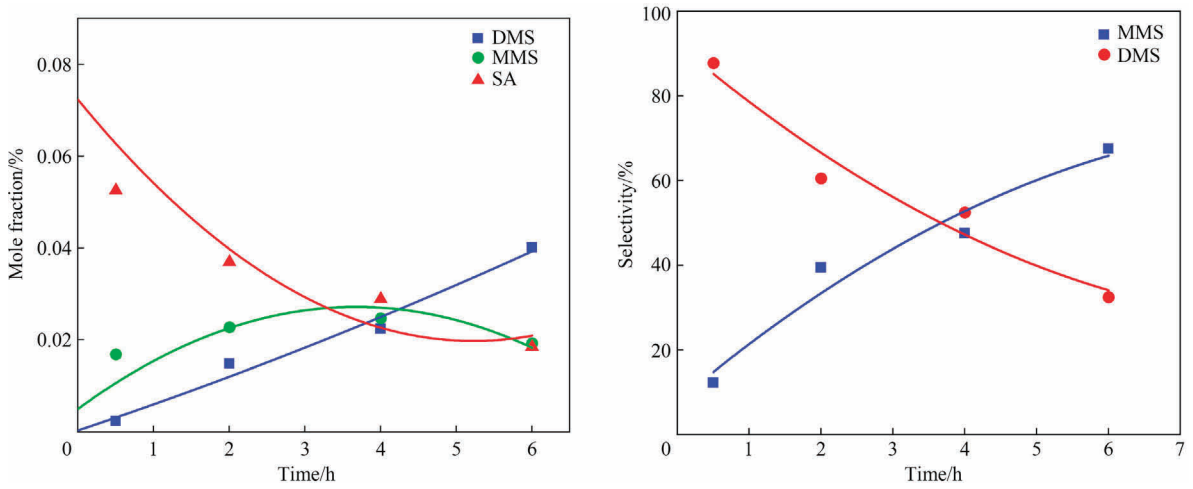

Fig. 5. The variation of main components with time in DSA esterification reaction (a) the variation of mole fraction with time; (b) time-dependent selectivity of DMS and MMS (reaction conditions: reaction temperature 170 °C, initial CO_2 pressure 1.0 MPa, DSA addition 1.0 mmol).

ther reacted with CH_3OH to form DMS. However, both MMS (Compound 5) and 4-methoxy-4-oxobutanoate (Compound 2) were observed in the reaction mixture from HRMS analysis. Therefore, there might be two possible reaction paths for the formation of DMS, similar to MMS generation. The theoretical calculation by Gaussian 16 software was also conducted for thermodynamics. At the reaction conditions of 140 °C and 3.1 MPa, the direct formation of DMS from the reaction of 4-methoxy-4-oxobutanoate (Compound 2) with CH_3OH was less possible as ΔG was 140.87 kJ·mol^{-1}. On the other hand, the reaction of MMS with CH_3OH was highly possible to generate DMS under the same reaction conditions given that the calculated ΔG was − 13.12 kJ·mol^{-1} in Eq. (7).

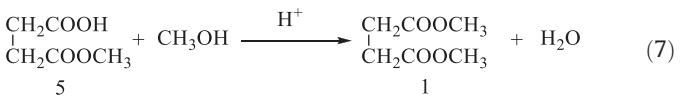

(7)

The common esterification between a carboxylic acid and alcohol is an equilibrium-limited reaction. To obtain a high yield of esters, it is necessary to remove the generated water from the reaction system, which could be achieved by chromatographic reactors [36] and reactive distillation [37]. Interestingly, the formed water could be immediately consumed by forming carbonic acid and then releasing H^+ during the direct esterification of disodium succinate, which would spontaneously expedite esterification and lead to negligible water content in the reaction mixture.

3.3. Kinetic modeling of DSA direct esterification

According to the results of HRMS analysis and the theoretical calculations, the reaction of DSA direct esterification possibly involved the first generation of sodium 3-carboxypropanoate, then forming MMS, and finally producing DMS, as summarized in Eqs. (1)–(7). For convenient kinetic modeling investigation, the major

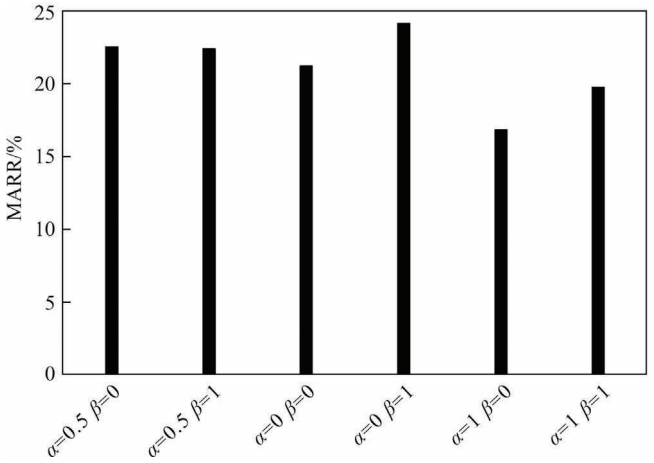

Fig. 6. The MARR values between the experimental data and the calculated values from the proposed kinetic models.

reaction route was therefore briefly described as exhibited in Eqs. (8) and (9).

$$CH_2COOH-CH_2COOH + CH_3OH \xrightarrow{H^+} CH_2COOH-CH_2COOCH_3 + H_2O \quad (8)$$

$$CH_2COOH - CH_2COOCH_3 + CH_3OH \xrightarrow{H^+} CH_2COOCH_3 - CH_2COOCH_3 + H_2O \quad (9)$$

To further verify the above proposed reaction pathways of DSA direct esterification, a detailed kinetic study was performed in the present work.

3.3.1. Kinetic model description

In a batch reactor, the changes in molar concentrations of components were expressed as follows:

$$-\frac{dc_A}{dt} = R_1 \quad (10)$$

$$-\frac{dc_B}{dt} = R_1 + R_2 \quad (11)$$

$$-\frac{dc_M}{dt} = -R_1 + R_2 \quad (12)$$

$$\frac{dc_E}{dt} = R_2 \quad (13)$$

$$\frac{dc_W}{dt} = R_1 + R_2 \quad (14)$$

where the subscript A, B, M, E and W represent DSA, CH_3OH, MMS, DMS and H_2O, respectively; R_1 and R_2 are the rate equations of Eqs. (8) and (9), respectively.

Table 3
Fitting results of reaction rate constants $k_1$and k_2 (α = 1, β = 0)

Temperature/℃	k_1/L^2·mol^{-2}·h^{-1}	k_2/L·mol^{-1}·h^{-1}
140	482.87	2.14
180	612.39	3.40
160	937.19	5.96
170	942.22	11.64

The rates of reactions (8) and (9) were assumed as to follow the power-law type:

$$R_1 = c_A^{\alpha}(k_1 c_A c_B) \quad (15)$$

$$R_2 = c_M^{\beta}(k_2 c_M c_B) \quad (16)$$

where k_1 and k_2 the reaction rate constants of Eqs. (8) and (9), respectively, and α and β as the adjustment coefficients, with a range of 0 to 1.

3.3.2. Determination of rate constants

The parameters of the proposed kinetic models consist of rate constants and adjustment coefficients. The kinetic models were fitted to the experimental data by using MATLAB software and the regression results were shown in Fig. 6. When α = 1 and β = 0, the average absolute deviation (MARR) between the experimental data and the calculated values from the kinetic models was 16.84%, which was the lowest among the kinetic models, as shown in Fig. 6. The obtained rate constants of the best fitted kinetic model were listed in Table 3. With the increased reaction temperature from 140 to 170 °C, the reaction rate of Eq. (8) increased rapidly from 482.87 to 937.19 L^2·mol^{-2}·h^{-1} and then slowly to 942.22 L^2·mol^{-2}•h^{-1}, while that of Eq. (9) increased steadily from 2.14 to 11.64 L·mol^{-1}·h^{-1}.

The temperature dependence of the rate constants k_i is evaluated according to the Arrhenius-type equation:

$$k_i(T) = A_i e^{-E_i/RT} \quad (17)$$

$$\ln k_i = \ln A_i - E_i/RT \quad (18)$$

where A_i is the pre-exponential factor, E_i is the activation energy (kJ·mol^{-1}), and R is the universal gas constant (J·mol^{-1}·K^{-1}). Thus, the activation energy and pre-exponential factor of each reaction could be obtained by the linear fitting of ln$k$ and 1/T. Fig. 7 showed the plot of lnk_1 and lnk_2 *versus* 1/T. The pre-exponential factors and the activation energies were obtained by linear fitting and presented in Table 4.

As shown in Table 4, the activation energies for MMS to react with methanol to form DMS was 85.80 kJ·mol^{-1}, which was obviously larger than that for DSA to form MMS. This meant that compared to the formation of MMS from DSA, the formation of DMS from MMS need to conquer a larger barrier. Considering α = 1 and β = 0, the consuming rate of DSA and the formation rate of DMS could thus be expressed as:

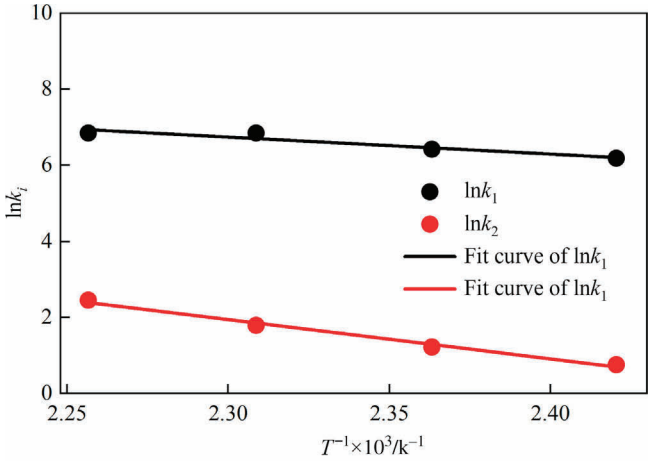

Fig. 7. The fitting curve of ln$k$ *vs.* 1/T for reaction.

Table 4
Fitting results of pre-exponential factors and activation energies

Rate constants	Parameters		R^2
	A_i	E_i	
k_1	2.46×10^7	37.15	0.91
k_2	1.41×10^{11}	85.80	0.99

$$r_{DSA} = -\frac{dc_A}{dt} = -2.45 \times 10^7 \times e^{-\frac{35.70\times10^3}{RT}} c_A^2 c_B \quad (19)$$

$$r_{DMS} = \frac{dc_E}{dt} = 1.41 \times 10^{11} \times e^{-\frac{85.80\times10^3}{RT}} c_M c_B \quad (20)$$

According to Eqs. (19) and (20), for the conversion of DSA to MMS, it could be considered as a second-order reaction for DSA, and a first-order reaction for methanol. As for the conversion of MMS to DMS, it was regarded as a first-order reaction for both MMS and methanol.

3.3.3. Model comparison with experiments

With the rate equations obtained by data regression, the best fitted model predicts the variation of composition of DSA, MMS and DMS with time during the reaction process of DSA direct esterification under different reaction temperatures, as shown in Fig. 8.

It could be seen clearly from Fig. 8 that at all the investigated temperatures, great agreement was observed between the experimental data and calculated values from the best fitted model. As shown in Fig. 8, the proposed model predicted that the mole fraction of DSA decreased rapidly at first and then decreased slowly at all the investigated temperatures along with the reaction, and the consumption rate of DSA was only accelerated a bit with the increasing reaction temperature. This was consistent with the fact that the barrier for DSA to react with methanol was not very high. The cases for the production of MMS and DMS got complicated under different reaction temperatures. As shown in Fig. 8(a) and (b), more MMS were formed than DMS at a temperature of 140 °C and 150 °C, and the mole fraction of MMS increased to a maximum value and that of DMS increased gradually with the increasing of reaction time. However, as reaction temperature increased to 160 °C and 170 °C, the mole fraction of MMS increased to a maximum value and then tended to decrease and that of DMS continuously increased. Especially, when the temperature reached 170 °C, more DMS were generated and the time for MMS reaching a maximum value was shortened. The fact could be attributed to that the energy barrier for the transformation of MMS to form DMS was more than twice larger than that for the transformation of DSA to form MMS. When the temperature increased to 160 °C or higher, the reaction for MMS to further form DMS with a higher barrier was accelerated more compared to that for DSA to form MMS. This means more MMS were consumed to further form DMS, which led to a lower net production of MMS and a higher production of DMS. According to the kinetic analysis, it was more difficult for MMS to further form DMS during the reaction of DSA direct esterification in comparison to the transformation of DSA to MMS. Therefore, in order to improve the reaction results, it encourages us to design a proper catalyst to lower the barrier of the transformation of DSA to MMS.

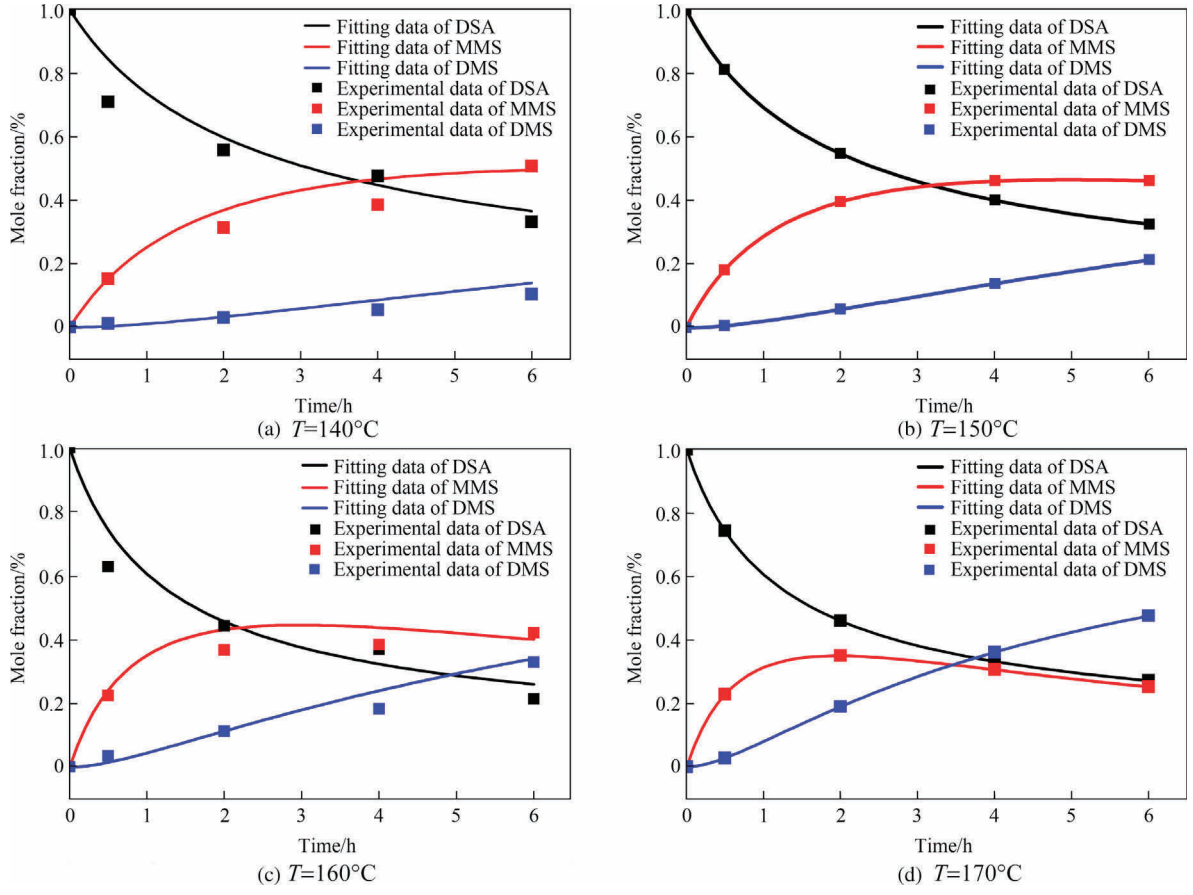

Fig. 8. Variation of the mole fraction of DSA, MMS and DMS with reaction time at different reaction temperatures (initial pressure of CO_2 was 1.0 MPa, initial dosage of DSA was 1.0 mmol).

4. Conclusions

The reaction pathway of DSA direct esterification with CO_2 and CH_3OH was determined by HRMS analysis of the reaction mixture and theoretical calculation. The results verified that CO_2 and CH_3-OH reacted to produce methyl carbonate for facilitating the esterification of DSA under the investigated reaction conditions. A detailed kinetic analysis was performed to further confirm the proposed reaction pathways. The activation energy for the reaction from DSA to MMS was 37.15 kJ·mol^{-1}, and 85.80 kJ·mol^{-1} for the reaction from MMS to DMS. In the future study, the conversion of monoester to diester could be accelerated by suitable catalysts.

Data Availability

Data will be made available on request.

Declaration of Competing Interest

The authors declare that they have no known competing financial interests or personal relationships that could have appeared to influence the work reported in this paper.

Acknowledgements

This work was financially supported by Natural Science Foundation of Shanxi Province (202203021221069 and 202103021223063); National Natural Science Foundation of China (21706172).

References

[1] C.C. Satam, M.J. Realff, Comparison of two routes for the bio-based production of economically important C4 streams, *J. Adv. Manuf. Process.* 2 (3) (2020) e10054.
[2] L.T. He, L. Liu, Y.Z. Huang, X.G. Miao, C. Len, Y.T. Wang, W.R. Yang, One-pot synthesis of dimethyl succinate from d-fructose using Amberlyst-70 catalyst, *Mol. Catal.* 508 (2021) 111584.
[3] L.L. Yao, H.F. Pan, W.J. Tian, T.C. Hui, Z.P. Xie, J.G. Zhang, Production of succinate by a metabolic engineered *Escherichia coli* and its scale-up process in fermentor, *Microbiol. China* 45 (12) (2018) 2541–2551.
[4] A. Mazière, P. Prinsen, A. García, R. Luque, C. Len, A review of progress in (bio)catalytic routes from/to renewable succinic acid, *Biofuels Bioprod. Biorefin.* 11 (5) (2017) 908–931.
[5] J.S. Lu, J.W. Li, H. Gao, D.W. Zhou, H.X. Xu, Y.X. Cong, W.M. Zhang, F.X. Xin, M. Jiang, Recent progress on bio-succinic acid production from lignocellulosic biomass, *World J. Microbiol. Biotechnol.* 37 (1) (2021) 1–8.
[6] M.I. Peñas, M. Criado-Gonzalez, A.M. de Ilarduya, A. Flores, J.M. Raquez, R. Mincheva, A.J. Müller, R. Hernández, Tunable enzymatic biodegradation of poly (butylene succinate): Biobased coatings and self-degradable films, *Polym. Degrad. Stab.* 211 (2023) 110341.
[7] J. Xu, B.H. Guo, Microbial Succinic Acid, Its Polymer Poly (butylene succinate), and Applications, in: G.Q. Chen (Ed.), Plastics from Bacteria, Springer, 2010.
[8] X.Y. Wan, D.Z. Ren, Y.J. Liu, J. Fu, Z.Y. Song, F.M. Jin, Z.B. Huo, Facile synthesis of dimethyl succinate *via* esterification of succinic anhydride over ZnO in methanol, *ACS Sustain. Chem. Eng.* 6 (3) (2018) 2969–2975.
[9] J. Xu, B.H. Guo, Microbial succinic acid, its polymer poly(butylene succinate), and applications, *Plastics from Bacteria: Natural Functions and Applications.* 14 (2010) 347–388.
[10] H. Shirahama, Y. Kawaguchi, M.S. Aludin, H. Yasuda, Synthesis and enzymatic degradation of high molecular weight aliphatic polyesters, *J. Appl. Polym. Sci.* 80 (3) (2001) 340–347.
[11] I. Bechthold, K. Bretz, S. Kabasci, R. Kopitzky, A. Springer, Succinic acid: A new platform chemical for biobased polymers from renewable resources, *Chem. Eng. Technol.* 31 (5) (2008) 647–654.
[12] A. Helal, R. Kreimerman, S. Gutiérrez, A.I. Torres, A market-driven algorithm for the assessment of promising bio-based chemicals, *AIChE J* 65 (12) (2019) e16775.
[13] S. Okino, R. Noburyu, M. Suda, T. Jojima, M. Inui, H. Yukawa, An efficient succinic acid production process in a metabolically engineered *Corynebacterium glutamicum* strain, *Appl. Microbiol. Biotechnol.* 81 (3) (2008) 459–464.
[14] S. D'Ambrosio, M. Ventrone, A. Alfano, C. Schiraldi, D. Cimini, Microbioreactor (micro-Matrix) potential in aerobic and anaerobic conditions with different industrially relevant microbial strains, *Biotechnol. Prog.* 37 (5) (2021) e3184.
[15] J. Wang, J.F. Zhu, G.N. Bennett, K.Y. San, Succinate production from different carbon sources under anaerobic conditions by metabolic engineered *Escherichia coli* strains, *Metab. Eng.* 13 (3) (2011) 328–335.
[16] A. Orjuela, A.J. Yanez, A. Santhanakrishnan, C.T. Lira, D.J. Miller, Kinetics of mixed succinic acid/acetic acid esterification with Amberlyst 70 ion exchange resin as catalyst, *Chem. Eng. J.* 188 (2012) 98–107.
[17] S.J. Lee, H. Song, S.Y. Lee, Genome-based metabolic engineering of *Mannheimia succiniciproducens* for succinic acid production, *Appl. Environ. Microbiol.* 72 (3) (2006) 1939–1948.
[18] C.S. López-Garzón, M. Ottens, L.A.M. van der Wielen, A.J.J. Straathof, Direct downstream catalysis: From succinate to its diethyl ester without intermediate acidification, *Chem. Eng. J.* 200–202 (2012) 637–644.
[19] C.S. López-Garzón, L.A.M. van der Wielen, A.J.J. Straathof, Green upgrading of succinate using dimethyl carbonate for a better integration with fermentative production, *Chem. Eng. J.* 235 (2014) 52–60.
[20] C.I. Cabrera-Rodríguez, L.A.M. van der Wielen, A.J.J. Straathof, Separation and catalysis of carboxylates: Byproduct reduction during the alkylation with dimethyl carbonate, *Ind. Eng. Chem. Res.* 54 (44) (2015) 10964–10973.
[21] B.A.V. Santos, V.M.T.M. Silva, J.M. Loureiro, A.E. Rodrigues, Review for the direct synthesis of dimethyl carbonate, *ChemBioEng Rev.* 1 (5) (2014) 214–229.
[22] L. Jeffry, M.Y. Ong, S. Nomanbhay, M. Mofijur, M. Mubashir, P.L. Show, Greenhouse gases utilization: A review, *Fuel* 301 (2021) 121017.
[23] S. Solomon, G.K. Plattner, R. Knutti, P. Friedlingstein, Irreversible climate change due to carbon dioxide emissions, *PNAS* 106 (6) (2009) 1704–1709.
[24] C.S. López-Garzón, L.A.M. van der Wielen, A.J.J. Straathof, Ester production from bio-based dicarboxylates via direct downstream catalysis: Succinate and 2, 5-furandicarboxylate dimethyl esters, *RSC Adv.* 6 (5) (2016) 3823–3829.
[25] U. Kamran, S.J. Park, Chemically modified carbonaceous adsorbents for enhanced CO_2 capture: A review, *J. Clean. Prod.* 290 (2021) 125776.
[26] A.H. Assen, Y. Belmabkhout, K. Adil, A. Lachehab, H. Hassoune, H. Aggarwal, Advances on CO_2 storage. Synthetic porous solids, mineralization and alternative solutions, *Chem. Eng. J.* 419 (2021) 129569.
[27] U. Savino, A. Sacco, Tandem devices for simultaneous CO_2 reduction at the cathode and added-value products formation at the anode, *J. CO2 Util.* 52 (2021) 101697.
[28] M. Zhang, Y.H. Xu, B.L. Williams, M. Xiao, S.J. Wang, D.M. Han, L.Y. Sun, Y.Z. Meng, Catalytic materials for direct synthesis of dimethyl carbonate (DMC) from CO_2, *J. Clean. Prod.* 279 (2021) 123344.
[29] B.A.V. Santos, C.S.M. Pereira, V.M.T.M. Silva, J.M. Loureiro, A.E. Rodrigues, Kinetic study for the direct synthesis of dimethyl carbonate from methanol and CO_2 over CeO_2 at high pressure conditions, *Appl. Catal. A* 455 (2013) 219–226.
[30] B.A.V. Santos, V.M.T.M. Silva, J.M. Loureiro, D. Barbosa, A.E. Rodrigues, Modeling of physical and chemical equilibrium for the direct synthesis of dimethyl carbonate at high pressure conditions, *Fluid Phase Equilib.* 336 (2012) 41–51.
[31] C.I. Cabrera-Rodríguez, L. Paltrinieri, L.C.P.M. de Smet, L.A.M. van der Wielen, A. J.J. Straathof, Recovery and esterification of aqueous carboxylates by using CO_2-expanded alcohols with anion exchange, *Green Chem.* 19 (3) (2017) 729–738.
[32] P.P. Barve, S.P. Kamble, J.B. Joshi, M.Y. Gupte, B.D. Kulkarni, Preparation of pure methyl esters from corresponding alkali metal salts of carboxylic acids using carbon dioxide and methanol, *Ind. Eng. Chem. Res.* 51 (4) (2012) 1498–1505.
[33] K.N. West, C. Wheeler, J.P. McCarney, K.N. Griffith, D. Bush, C.L. Liotta, C.A. Eckert, *In situ* formation of alkylcarbonic acids with CO_2, *Chem. A Eur. J.* 105 (16) (2001) 3947–3948.
[34] J.L. Gohres, A.T. Marin, J.E. Lu, C.L. Liotta, C.A. Eckert, Spectroscopic investigation of alkylcarbonic acid formation and dissociation in CO_2-expanded alcohols, *Ind. Eng. Chem. Res.* 48 (3) (2009) 1302–1306.
[35] A.K. Kolah, N.S. Asthana, D.T. Vu, C.T. Lira, D.J. Miller, Reaction kinetics for the heterogeneously catalyzed esterification of succinic acid with ethanol, *Ind. Eng. Chem. Res.* 47 (15) (2008) 5313–5317.
[36] D.S.M. Constantino, C.S.M. Pereira, R.P.V. Faria, A.F.P. Ferreira, J.M. Loureiro, A. E. Rodrigues, Synthesis of butyl acrylate in a fixed-bed adsorptive reactor over Amberlyst 15, *AIChE J.* 61 (4) (2015) 1263–1274.
[37] W.T. Han, Z.W. Han, X.C. Gao, Z. Hong, X.G. Li, H. Li, X.H. Gu, X. Gao, Inter-integration reactive distillation with vapor permeation for ethyl levulinate production: Equipment development and experimental validating, *AIChE J.* 68 (2) (2022) e17441.